Model Based Correction of Triggered MR Thermometry for LITT

J. P. Yung[1,2], F. Maier[3], D. Fuentes[1], A. J. Krafft[3], A. Elliott[1], M. Bock[3], J. D. Hazle[1,2], W. Semmler[3], and R. J. Stafford[1,2]
[1]Department of Imaging Physics, University of Texas M.D. Anderson Cancer Center, Houston, TX, United States, [2]The University of Texas Graduate School of Biomedical Sciences, Houston, TX, United States, [3]Medical Physics in Radiology, German Cancer Research Center (DKFZ), Heidelberg, Germany

Introduction

During MR-guided therapies, MR temperature imaging (MRTI) quantitatively monitors the induced temperature changes. When used with a real-time feedback, the extent of tissue damage during the delivery of the thermal energy can be estimated, and thus, enable a safer and more conformal therapy [1]. The proton resonance frequency (PRF) shift technique is the most widely used MRTI technique, but can be corrupted by complications induced from tissue motion.

In this work, a triggered segmented EPI pulse sequence [2] was used for PRF temperature imaging in the same position during nearly periodic motion of the tissue. A Pennes bioheat transfer based Kalman filter using MRTI input provided temperature estimates at instances when the triggered sequence failed due to large, non-periodic motion during the therapy delivery.

Materials and Methods

PRF temperature mapping was performed on a clinical 1.5T whole body MR system (Espree, Siemens, Erlangen, Germany) using a large flex loop coil. A segmented EPI sequence (TR = 27 ms; TE = 15 ms; α = 17°; FOV = 200×200 mm; matrix = 128×128; slice thickness = 5 mm; EPI factor = 11; BW = 870 Hz/px; Navigator update rate = 18.5 Hz) was developed for triggered temperature mapping [2]. For tissue heating, an *ex vivo* liver embedded in agarose gel was exposed to a 980-nm laser irradiation (4W for ~5.5 min) using a 1-cm diffusing-tip fiber (BioTex, Inc, Houston, TX). During the experiment, temperature changes were monitored (Fig. 1) using a thermal ablation monitoring software (*TAM*) developed in-house [3].

To mimic abdominal breathing motion, the phantom was manually moved along the direction of the MRI bore 3-4 cm every 5 s. A 1D Kalman-filtered velocity navigator triggering sequence was used to synchronize image acquisitions to the motion of the phantom (Fig. 2). However, in unique situations during the experiment, the motion of the phantom did not follow the assumed sinusoidal motion, resulting in corruption of the MRTI data. Based on empirical observation, a velocity navigator value of 2 cm/s or greater preceding or following an MRTI acquisition was chosen as the threshold for the data to be ignored.

A Pennes bioheat transfer based Kalman filter using the MRTI input was used for predicting temperatures during therapy delivery in the presence of noise. The Kalman algorithm [4] provided an uncertainty weighted temperature estimate throughout the treatment using a combination of the MRTI feedback and a linear stochastic differential form of the Pennes bioheat transfer model [5], using literature values [6], which were approximated to first order as remaining homogenous in the delivery region. A model covariance error of 1 was used in the Kalman filter.

Results and Discussion

From acquisitions prior to heating, the velocity navigator triggered sequence obtained a temperature uncertainty of 1.8 °C. During the experiment, the velocity before or after a MRTI acquisition exceeded 2 cm/s 9 times. In these cases, the temperature images were corrupted and resulted in temperature artifacts. When following the time course of a voxel adjacent to and further away from the fiber (cf. Fig. 3), large deviations from the normal heating and cooling curves were observed (Fig. 4). During thermal therapies, these outliers could interfere with monitoring of the therapy and prediction of the outcomes. However, using the navigator for both triggering and determination of data to be rejected and replaced with a Kalman filtered estimate eliminated large sudden changes and provided smoother heating and cooling curves. The Kalman estimates also showed good agreement with areas in the MRTI data where temperature changes were small indicating the underlying information being kept intact while reducing temperature variations from any triggering imprecision. Temperature uncertainty prior to heating for the Kalman estimates was measured to be 0.80 °C. More sudden changes in the MRTI data are expected to not affect the effectiveness of the Kalman filtered temperatures estimates as the loss of data only exists for brief periods of time before recovering. However, relying solely on the temperature model for an extended amount of time would result in erroneous heat distributions due to model inaccuracies.

In this phantom study, sudden or extreme motions where navigation failed were detected using the navigation and corrected for with the use of a temperature model-based Kalman filter of the MRTI input. The combination of the two techniques may facilitate continuous, accurate temperature monitoring in the presence of motion allowing for increased safety and efficacy for thermal therapies. While this technique does not correct for implicit errors in the temperature imaging, such as from susceptibility, it does provide a more optimal estimate of the missing data. Studies quantifying the relationship between the velocity triggered measurements and the threshold for data rejection, as well as methods for better quantifying the effectiveness of this approach are ongoing.

References

[1] Carpentier, A., et al. Neurosurgery, 2008. 63(1).; [2] Maier F. et al. 8th IMRI Symposium, Leipzig, 2010.; [3] Maier F. et al. IFMBE Proc. 25, 2009.; [4] Kalman, R.E., J. Basic Engineer., 1960. 82(1).; [5] Pennes, H.H, J. Appl. Physio., 1948. 1.; [6] Kreith & Goswami, CRC Handbook 2004.

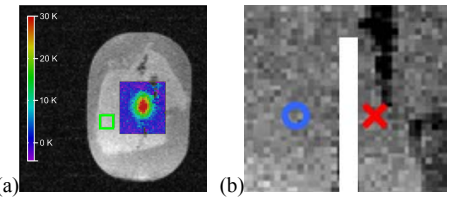

Fig. 1: (a) Magnitude image of *ex vivo* phantom with an overlaid ROI showing temperature rise in Kelvins (left). Phase drift was corrected using the mean temperature within green square. (b) Markers showing location of measured voxels relative to the laser fiber (right).

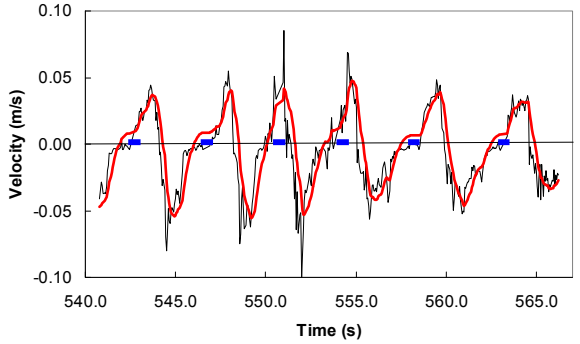

Fig. 2: Example of temporal navigator velocity estimations with measured (black) and Kalman-filtered (red) velocities. Image acquisitions are indicated by blue bars.

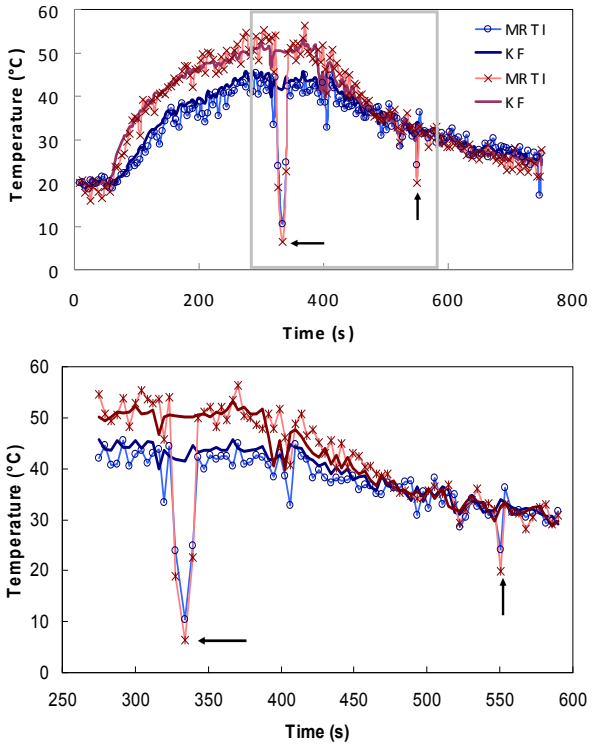

Fig. 4: Temperature evolution of voxels (top) with solid lines showing Kalman-filtered estimates and a close up (bottom) of temperature deviations (arrows) corrected by the temperature model-based Kalman.